Published in final edited form as:
*J Gerontol A Biol Sci Med Sci*. 2006 March ; 61(3): 245–255.

# Molecular Regulation of Apoptosis in Fast Plantaris Muscles of Aged Rats

**Emidio E. Pistilli**, **Parco M. Siu**, and **Stephen E. Alway**
Laboratory of Muscle Biology and Sarcopenia, Division of Exercise Physiology, West Virginia University School of Medicine, Morgantown.

## Abstract

This study tested the hypothesis that aging exacerbates apoptotic signaling in rat fast plantaris muscle during muscle unloading. Plantaris muscle mass was 22% lower in aged animals and the apoptotic index was 600% higher, when compared to those in young adult animals. Following 14 days of hind-limb unloading, absolute plantaris muscle mass was 20% lower in young adult animals with a corresponding 200% higher elevation of the apoptotic index. Unloading had no affect on muscle weight or apoptotic index of aged plantaris muscles. The changes in proapoptotic messenger RNA (mRNA) for apoptotic protease activating factor-1 (Apaf-1), Bax, and inhibitor of differentiation protein-2 (Id2) were exacerbated with aging. Bax and Bcl-2 protein levels were also altered differently in aged muscle, compared to young. Significant positive correlations were observed between the changes in Id2 and Bax mRNA, and Id2 and caspase-9 mRNA. These data suggest that a pro-apoptotic environment may contribute to aging-associated atrophy in fast skeletal muscle, but apoptotic signaling differs by age.

Muscle mass and strength are reduced as a result of aging, a condition known as sarcopenia (1-5). Sarcopenia contributes to a loss of independence with advanced age and increases the risk of falling in elderly persons (5). This is an important problem because hypokinesia is profound in older populations, and aging increases the sensitivity of muscle fibers to inactivity-induced atrophy (6-9). Thus, it appears possible that superimposing disuse or immobility with sarcopenia (e.g., recovery from surgery or a fall) may further exacerbate the loss of muscle mass and strength.

Limb unloading is a common means to induce atrophy in skeletal muscles. In rodents, this is usually achieved by hind-limb suspension (HS; 10-15) or immobilization (16). HS is a model of simulated microgravity that has been used to investigate skeletal muscle adaptations during nonweight-bearing conditions (17). The rapid loss of muscle fiber cross-sectional area during unloading indicates that the atrophying myofibers have activated pathways leading to decreased rates of protein synthesis and increased degradation of myofibrillar proteins (18, 19). The atrophy of antigravity hind-limb muscles, especially the soleus, is quite severe (11, 20-22) and is associated with a down-regulation of slow myosin heavy chain expression (23) and a decrease in the number of nuclei per muscle fiber (22). Furthermore, an increase in TUNEL (terminal deoxynucleotidyl transferase biotin-dUTP nick end labeling)-positive nuclei in slow rat skeletal muscle have been reported after HS leading to muscle atrophy as compared to control muscles (11). Recent reports have also demonstrated increases in proapoptotic



Address correspondence to Stephen E. Alway, PhD, Laboratory of Muscle, Sarcopenia and Muscle Diseases, Division of Exercise Physiology, West Virginia University School of Medicine, Robert C. Byrd Health Science Center, Morgantown, WV 26506-9227. salway@hsc.wvu.edu.

proteins involved in the mitochondria-associated apoptotic pathway in the soleus muscle (24), and in the mixed fiber medial gastrocnemius muscle, as a result of both aging and limb unloading (25). These data suggest that some of the nuclei were lost via apoptosis. Nevertheless, much less is known about the predominately fast fiber containing plantaris muscle, where muscle mass losses are less severe as a result of aging and unloading (10,12, 16,26).

The degree of apoptosis depends on the balance between the activation of pro- and anti-apoptotic genes. In general, shifts in this balance toward increasing pro-apoptotic genes are believed to promote muscle atrophy (27). Pro-apoptotic markers involved in the mitochondria-associated apoptotic pathway in skeletal muscle can take part in a caspase-dependent or a caspase-independent pathway. The caspase-dependent pathway is initiated by the release of cytochrome *c* from the mitochondria intermembrane space which then forms a complex with apoptotic protease activating factor-1 (Apaf-1), 2′deoxyodenosine 5′-triphosphate (dATP), and pro-caspase-9 (27-29), leading to the activation of caspase-9 and other downstream caspases. In contrast, the caspase-independent pathway involves apoptosis-inducing factor (AIF), which can translocate to the nucleus and initiate chromatin condensation and DNA fragmentation (30,31). The release of these pro-apoptotic molecules is controlled by the BCL-2 family of proteins, with Bax and Bak promoting apoptosis and Bcl-2 inhibiting apoptosis (27). We have recently proposed a role for inhibitor of differentiation (Id) repressors in skeletal muscle apoptosis and sarcopenia (32). Id levels are correlated with muscle wasting (33), and we and others have shown increases in markers of apoptosis in muscles of aged animals (32,34,35). Because we have found high levels of inhibitor of differentiation protein-2 (Id2) in the atrophic muscles of aged rodents (32,33), we were interested in determining if Id2 might be involved in general pathways leading to apoptosis in muscle during periods of unloading, especially in aged animals.

The biochemical signals regulating apoptosis during aging and unloading, especially in fast skeletal muscles, have not been well studied. Therefore, in the current study we examined Id2 and molecular markers of apoptosis in experimentally unloaded muscles of young adult and aged Fischer 344 × Brown Norway (FBN) rats, to determine if these conditions influence the degree of muscle atrophy via apoptotic pathways. We hypothesized that plantaris muscles from aged animals would exhibit increases in markers for apoptosis and that these changes would be exacerbated following HS. We therefore tested the hypothesis that plantaris muscles from young adult rats would not have marked elevations in messenger RNA (mRNA) levels for Id2 and pro-apoptotic genes, whereas muscles from aged rats would have increased mRNA levels of Id2 and proapoptotic genes that would be further altered following hind-limb unloading.

## METHODS

### Animal Care and HS

All procedures followed the guidelines of the National Institutes of Health, and were approved by the Institutional Animal Care and Use Committee of the West Virginia University School of Medicine. Sixteen young adult (9 month) and 16 senescent (33 month) male FBN rats were obtained from the National Institute on Aging barrier-raised colony that is housed at Harlan Animal Colonies (Indianapolis, IN). The animals were housed at 20–22°C in barrier-controlled conditions under a 12-hour light/dark cycle. They were provided rat chow and water ad libitum.

The rats in each age group were randomly assigned to an HS group ($n = 8$) or a control group ($n = 8$). The HS animals were unloaded using the methods described previously (17) with modifications. Briefly, an adhesive (tincture of benzoin) was applied to the tail and allowed to dry. Orthopedic tape was applied along the proximal one third of the tail, which distributed the load evenly and avoided excessive tension on a small area. The tape was placed through a wire

harness that was attached to a fish line swivel at the top of a specially designed HS cage. This provided the rats with 360° of movement around the cage. Sterile gauze was wrapped around the orthopedic tape and was subsequently covered with a thermoplastic material, which formed a hardened cast (Vet-Lite; Veterinary Specialty Products, Boca Raton, FL). The exposed tip of the tail remained pink, indicating that HS did not interfere with blood flow to the tail. The suspension height was monitored daily and adjusted to prevent the hind limbs from touching any supportive surface, with care taken to maintain a suspension angle of approximately 30° (17). The forelimbs maintained contact with a grid floor, which allowed the animals to move, groom themselves, and obtain food and water freely. HS was maintained for a total of 14 days. Control rats maintained normal mobility, and they moved unconstrained around their cages. Following 14 days of HS, rats were killed with an overdose of xylazine, and the plantaris muscles from the hind limb were excised.

## Reverse Transcription–Polymerase Chain Reaction Estimates of mRNA

Semiquantitative reverse transcription–polymerase chain reaction (RT–PCR) analysis was conducted as described in detail elsewhere (25). Frozen muscle samples (≈50 mg) were homogenized in 1 ml of TriReagent (Molecular Research Center, Cincinnati, OH) with a mechanical homogenizer. Total RNA was isolated by centrifugation and washed in ethanol according to the manufacturer's instructions. RNA was solubilized in 20 μl of RNase-free $H_2O$. RNA was treated with Dnase I (Ambion, Austin, TX) and reverse transcribed (RT) with random primers (Invitrogen/Life Technologies, Bethesda MD).

Primers were constructed from published sequences (Table 1). Primer pairs for the gene of interest were coamplified with 18S primer pairs and competimers to the 18S primers, as an internal control, according to the manufacture's protocols (Ambion). The number of PCR cycles was determined for each gene to insure that analyses were done in the linear range of amplification. The signal from the gene of interest was expressed as a ratio to the 18S signal from the same PCR product to eliminate any loading errors. The complementary DNA from all muscle samples was amplified simultaneously for a given gene. Following amplification, 20 μl of each reaction was subjected to electrophoresis on 1.5% agarose gels. Gels were stained with ethidium bromide. PCR signals were captured with a digital camera (Kodak 290; Eastman Kodak Company, Rochester, NY), and the signals were quantified using Kodak image analysis software (Eastman Kodak) in arbitrary units as optical density (OD) × band area.

## Protein Measures

Frozen muscle samples were used to obtain cytoplasmic protein to be used in western blots. Muscle samples, approximately 50–75 mg, were homogenized in 1 ml of ice-cold lysis buffer (10 mM NaCl, 1.5 mM $MgCl_2$, 20 mM HEPES at pH 7.4, 20% glycerol, 0.1% Triton X-100, and 1 mM dithiothreitol) to obtain cytoplasmic protein extracts according to the methods of Rothermel and colleagues (36). Muscle homogenates were centrifuged at 3000 rpm for 5 minutes at 4°C. The supernatants that contained the cytoplasmic protein fraction were collected. The protein concentration of the total muscle homogenate was assayed spectrophotometrically at 562 nm (SmartSpec 3000; Bio-Rad Laboratories, Hercules, CA) using a commercial bicinchoninic acid (BCA) method as recommended by the manufacturer (Pierce, Rockford, IL) with bovine serum albumin used as standard. Fifty micrograms of cytoplasmic protein was loaded into each lane of a 12% polyacrylamide gel and separated by routine sodium dodecyl sulfate–polyacrylamide gel electrophoresis (SDS–PAGE) for 1.5 hours at 20°C. Separated proteins were transferred to nitrocellulose membranes, and verification of equivalent protein loading and transfer was verified by Ponceau S red (Sigma, St. Louis, MO). The membranes were blocked at room temperature for 1 hour in 5% nonfat milk in Tris-buffered saline containing 0.05% Tween (TBS-T). Membranes were probed with anti-Bcl-2 mouse monoclonal antibody (1:200 dilution, sc-7382; Santa Cruz Biotechnology),

and anti-Bax rabbit polyclonal antibody (1:200 dilution, sc-6236; Santa Cruz Biotechnology) diluted in TBS-T with 2% nonfat milk. Secondary antibodies were conjugated to horseradish peroxidase (HRP; Chemicon International, Temecula, CA), and signals were developed using a chemiluminescent substrate (ECL Advanced; Amersham Biosciences, Piscataway, NJ). Signals were visualized by exposing the membranes to x-ray films (BioMax MS-1; Eastman Kodak). Digital records were captured by a Kodak 290 camera, and protein bands were quantified using 1-D image analysis software (Eastman Kodak). Bands were quantified as OD × band area and were expressed as arbitrary units.

### Cell Death Enzyme-Linked Immunosorbent Assay and Calculation of Apoptotic Index

Cytoplasmic protein extracts were used to quantify DNA fragmentation in all muscle samples using a commercially available enzyme-linked immunosorbent assay (ELISA) kit (Cell Death Detection ELISA; Roche Diagnostics, Mannheim, Germany). Briefly, the wells of a 96-well plate were coated with a primary anti-histone mouse monoclonal antibody. Following the addition of 100 μl of each sample, a secondary anti-DNA mouse monoclonal antibody coupled to peroxidase was added to each well. The substrate, 2,2′-azino-di-(3-ethylbenzthiazoline sulfonate) (ABST) was used to photometrically determine the amount of peroxidase retained in the immunocomplex. The color change of each well was determined at a wavelength of 405 nm using a Dynex MRX plate reader and computer software (Revelation; Dynatech Laboratories, Chantilly, VA). The resulting OD was normalized to the protein concentration of each sample and recorded as the apoptotic index ($OD_{405} \cdot mg\ protein^{-1}$).

### In Situ TUNEL

Apoptotic nuclei of myogenic origin were assessed using a fluorometric TUNEL detection kit according to the manufacture's instructions (Roche Applied Science, Indianapolis, IN). Frozen 10-μm-thick muscle cross-sections of the medial gastrocnemius muscle from control young and aged rats were cut in a cryostat at −22° and placed on the same glass slide to control for differences in tissue processing. Muscle characteristics and apoptotic data from the medial gastrocnemius muscle have been described previously (25). Slides were air dried, fixed in 4% paraformaldehyde in phosphate-buffered saline (PBS) at room temperature, permeabilized in 0.2% Triton X-100 in 0.1% sodium citrate at 4°C for 2-minutes, and incubated in TUNEL reaction mixture in a humidified chamber at 37°C for 1 hour in the dark. Negative control experiments were performed in which the terminal deoxynucleotidyl transferase (TdT) enzyme was not added to the TUNEL reaction mixture. Sections were then incubated in an anti-laminin mouse monoclonal antibody followed by an anti-mouse immunoglobulin G Cy3 conjugate F (ab′)2 fragment incubation (1:200 dilution, C2182; Sigma). Sections were mounted with 4′,6-diamidino-2-phenylindole (DAPI) mounting medium (Vectashield mounting medium; Vector Laboratories). Images were visualized using an epifluorescence microscope at an objective magnification of 40x and at the following excitation wavelengths: 330–380 nm for DAPI blue fluorescence, 450–490 nm for green fluorescence, and 485–585 nm for Cy3 red fluorescence. Images were obtained using a SPOT RT camera (Diagnostic Instruments, Sterling Heights, MI), and SPOT RT software (Universal Imaging, Downingtown, PA) was used to superimpose the images.

### Immunofluorescence Staining

Frozen 10-μm-thick muscle cross-sections of the medial gastrocnemius muscle from control young and aged rats were cut in a cryostat at −22° and placed on the same glass slide to control for differences in tissue processing. Slides were air dried at room temperature and fixed in ice-cold acetone/methanol (50:50), permeabilized in 0.2% Triton X-100 in 0.1% sodium citrate at 4°C for 5 minutes, and blocked in 1.5% normal goat serum at room temperature for 15 minutes in a humidified chamber. A double-label protocol was used to visualize pro-apoptotic Bax

protein as well as the basal lamina of individual muscle fibers. After washing in PBS, sections were incubated in an anti-Bax rabbit polyclonal antibody (1:20 dilution, SC-; Santa Cruz Biotechnology, Santa Cruz, CA) followed by addition of an antirabbit fluorescent antibody. The tissue sections were washed in PBS and then incubated in antilaminin mouse monoclonal antibody (2E8; Hybridoma Bank, Iowa City, IA) followed by an anti-mouse immunoglobulin G Cy3 conjugate F(ab′)2 fragment incubation (1:200 dilution, C2182; Sigma). Sections were mounted with DAPI mounting medium (Vectashield mounting medium; Vector Laboratories). Images were visualized under a Nikon SE800 fluorescence microscope at an objective magnification of 40× and at the following excitation wavelengths: 330–380 nm for DAPI blue fluorescence, 450–490 nm for green fluorescence, and 485–585 nm for Cy3 red fluorescence. Images were obtained using a SPOT RT camera (Diagnostic Instruments), and SPOT RT software (Universal Imaging) was used to merge all images.

### Statistical Analysis

Statistical analyses were performed using the SPSS software package, version 10.0. Data were examined using a two-way analysis of variance to analyze the main effects of age and unloading and the Age × Unloading interaction with significance set at $p < .05$. Group differences were examined using a one-way analysis of variance and Tukey's post hoc test. Data are presented as means ± standard error (*SE*). Relationships between given variables were examined by computing the Pearson correlation coefficient.

## RESULTS

### Body Weight

Body weight was higher in aged rats than in young adult rats (aged control, 539 ± 16 g; young adult control, 374 ± 25 g). Two weeks of HS significantly reduced body weights by 21% in young adult rats (295 ± 13) and by 15% in aged rats (457 ± 11 g), respectively.

### Muscle Characteristics

In aged rats, the absolute plantaris muscle wet weight was 22% lower than that in young adult rats (Figure 1A). When muscles were normalized to bodyweight, plantaris muscles from aged rats were 47% less than muscles from young adult rats, suggesting a preferential loss of muscle mass with aging (Figure 1B). Following 2 weeks of HS, the absolute wet weight of plantaris muscles from young adult rats was 20% lower than that from young adult control rats. In contrast, 2 weeks of HS had no effect on the absolute wet weight of plantaris muscles from aged rats, when compared to aged controls (Figure 1A). Muscle protein content was 29% lower in aged plantaris muscles compared to young adult plantaris muscles, suggesting increases in protein degradation and/or decreases in protein synthesis as a result of advanced age. Two weeks of HS did not significantly affect muscle protein content in the plantaris muscles in either young adult or aged rats (Figure 1C).

### Apoptotic Index and Fluorescent TUNEL Assay

The cell death ELISA showed a higher apoptotic index (600%) in plantaris muscles from aged rats when compared to young adult rats. Following 2 weeks of HS, the apoptotic index was 200% higher in plantaris muscles from young adult rats compared to muscles from young adult control rats. In contrast, 2 weeks of HS did not affect the apoptotic index in aged plantaris muscles, when compared to aged control muscles (Figure 2A). Fluorescent images demonstrated the presence of apoptotic TUNEL-positive nuclei under the basal lamina in aged muscles, whereas young adult muscles showed very few TUNEL-positive nuclei (Figure 2B and C).

### mRNA and Protein Alterations in the Bcl-2 Family Markers

In the current study, the mRNA and protein contents of Bax and Bcl-2 were measured as markers promoting and attenuating apoptosis, respectively (Figure 3). As a result of aging, Bax mRNA and protein content, and Bcl-2 protein content were higher in aged plantaris muscles when compared to young adult control muscles. Following 2 weeks of HS, Bax mRNA was 120% and 25% higher in young adult and aged plantaris muscles, respectively (Figure 3A). Bcl-2 mRNA and protein content were 44% lower and 200% higher in young adult plantaris muscles following HS and 61% and 110% higher in aged plantaris muscles following HS (Figure 3C and D). Fluorescent images also demonstrated intense cytoplasmic staining for pro-apoptotic Bax protein in muscle fibers from aged animals, whereas staining was very faint and often not detectable in fibers from young adult muscles (Figure 4A and B).

### mRNA Alterations of Apoptotic Genes

Specific pro-apoptotic markers involved in the mitochondria-associated apoptotic pathway were examined for their contribution to changes observed in young and aged plantaris muscles (Figure 5). As a result of aging, Id2 mRNA was 100% higher in aged plantaris muscles when compared to young adult control muscles. When normalized to control muscles, Id2 mRNA was unchanged in young adult plantaris muscles following HS, but was 110% higher in aged plantaris muscles following HS compared to aged control muscle (Figure 5A). Following 2 weeks of HS, AIF mRNA was higher in young adult and aged plantaris muscles than in control muscles (Figure 5B). The pro-apoptotic marker Apaf-1 was 120% higher in aged plantaris muscles following HS (Figure 5C). Caspase-9 mRNA was not affected by 2 weeks of HS in young adult or aged muscles (Figure 5D).

### Relationships Between Markers of Apoptosis

The relationships of these apoptotic markers were analyzed by computing the Pearson correlation coefficient. Significant positive correlations were observed between Id2 and Bax mRNA ($r = 0.716$, $p = .002$) (Figure 6A), and Id2 and caspase-9 mRNA ($r = 0.500$, $p = .049$) (Figure 6B).

## DISCUSSION

The normal aging process is associated with a reduction in muscle mass and strength (sarcopenia) (1-5) which can be exacerbated with reduced activity patterns (6-8,14). In this study, we sought to determine if apoptosis contributed to the muscle atrophy observed in fast fiber containing muscles as a result of aging, and if reduced activity (HS) influenced these apoptotic changes. The present study demonstrates that muscle atrophy of the plantaris muscle, via the aging process, is partly mediated by increases in the presence of apoptosis, and that inactivity can exacerbate the alterations in some of the markers examined, specifically Id2 and Apaf-1. Further, young adult plantaris muscles show elevations in the mitochondria apoptotic pathway following HS, and these changes are similar to those observed in aged control plantaris muscles. To our surprise, superimposing HS with aging did not stimulate further losses of muscle mass in the plantaris muscle, as has been shown previously in the soleus muscle (24) and the medial gastrocnemius muscle (25). These results in the fast fiber plantaris muscle warrant further investigation, as muscle loss via unloading and via sarcopenia involve differing processes that may affect the degree of atrophy observed.

### Apoptotic Pathways Contribute to Sarcopenia

This study attempted to simulate sarcopenia and hypokinesia that is commonly observed in elderly humans by using a rodent model of unloading in young adult and aged animals. The contribution of apoptotic processes to the myonuclear and myofiber loss observed with aging

is actively being investigated and still remains to be fully elucidated. This study provides evidence that aging-related muscle loss is associated with an increase in pro-apoptotic processes. The main effect of aging on muscle atrophy ( $p < .001$) and the incidence of apoptosis ( $p < .001$) were both highly significant, as the aged control plantaris muscles were lighter than young control muscles when expressed either as absolute muscle weight (22%) or normalized to body weight (47%), and the apoptotic index was 600% higher in aged plantaris muscles. Apoptotic nuclei, identified through TUNEL staining, were also visualized under the basal lamina indicating significant nuclear apoptosis in aged skeletal muscle. These data support previous findings of elevated apoptosis in the predominately slow fiber containing soleus muscle (24) and the mixed fiber containing gastrocnemius muscle (25) with aging, and suggest that an apoptotic program is conserved across muscles of differing fiber type and activity patterns.

Although the role of apoptosis in mature skeletal muscle remains poorly understood, it has been suggested that aged skeletal muscle has a greater potential to undergo apoptotic processes (24). Leeuwenburgh and colleagues (24) demonstrated specific elevations of EndoG, a caspase-independent marker, in aged soleus muscles. In the present study, the basal levels of pro-apoptotic Bax mRNA and protein in aged plantaris muscles were more than double those of young adult plantaris muscles, supporting previous findings from our laboratory in the medial gastrocnemius muscle (25). Additionally, fluorescent images revealed a widespread cytoplasmic localization of Bax protein in aged skeletal muscle, compared to young muscle. These increases in pro-apoptotic markers within aged skeletal muscle could potentially enhance muscle loss following a further apoptotic stimulus. Interestingly, aged skeletal muscle also seems to undergo adaptations to counteract this increased apoptotic potential by up-regulating anti-apoptotic proteins, such as Bcl-2. Although this attempt is largely overruled, it highlights the differences inherent in aged skeletal muscle when compared to that of young adults.

## Differences in Unloading-Induced Apoptosis With Age

The results of this study show that, in response to unloading, aged plantaris muscles induce a molecular program favoring apoptosis that differs from young adult plantaris muscle. Aged plantaris muscles initiated an up-regulation of Apaf-1 mRNA in response to HS with no increases observed in the young tissue. Pro-apoptotic Bax mRNA and protein were increased to a greater extent in plantaris muscles from young adult rats following HS, when compared to aged rats. However, this effect was due to a greater basal level of Bax in the aged control plantaris muscle. These data suggest an increase in apoptosis via the caspase-dependent pathway and that components of the mitochondria-associated apoptotic pathway are regulated at the pretranslational level differently with age. An interesting finding of this study was the increase in anti-apoptotic Bcl-2 mRNA and protein in the aged plantaris muscle following HS, supporting previous findings in our laboratory in the medial gastrocnemius muscle (25) and when using an avian model of unloading (37). Bcl-2, a member of the BCL-2 family, opposes mitochondria-mediated apoptosis by inhibiting cytochrome *c* release from the mitochondria (27). Young adult plantaris muscle showed a reduced expression of Bcl-2 mRNA following unloading, suggestive of a proapoptotic environment. However, Bcl-2 mRNA and protein were 61% and 100% higher in aged plantaris muscles, respectively, following HS when compared to aged control muscles. This response is suggestive of an adaptation in aged skeletal muscle at the molecular level, possibly as an attempt to counteract unloading-induced apoptosis.

The lack of muscle atrophy in the aged plantaris muscle following HS was surprising and warrants further investigation. Although these data conflict with previous data from our laboratory (10,12), they are consistent with data published by Thompson and colleagues (14). Following 1 week of HS in 30-month-old FBN rats, Thompson and colleagues (14) reported nonsignificant reductions in both absolute and relative plantaris muscle mass. Animal-to-

animal variability, environmental disturbances, and differences in unloading techniques could potentially alter the physiological response to HS (16). The 22% lower muscle weight in control muscles of the old rats in our current study as compared to the young adult rats represented sarcopenia, rather than any change over the 14 days of the study. The loss in muscle due to HS was not statistically significant (−12%) in the aged rats, but the HS-induced muscle loss was significant (−20%) in the plantaris of young adult rats. These HS-associated losses in muscle mass represent "real" losses of muscle, rather than a failure to grow during 14 days of the experimental manipulation. We base these conclusions on observations made in another pilot study (Alway SE and Chen KD, unpublished data, 1998) in rats that were 6 months and 33 months of age. In this cohort, body weight increased by 6.3 ± 1.3% and −0.8 ± 0.2 % over 14 days in caged control young adult and old rats, respectively. In this pilot study we found that plantaris muscle weight did not change (increase of 1.6%) in young adult rats (6 months of age) confined to their cages for 14 days as compared to rats that were killed 14 days earlier (i.e., at day 0). We would not expect that the 9-month-old rats in our current study would grow more rapidly than would the 6-month-old rats evaluated in this pilot study, so it is unlikely that significant muscle growth occurred in the 9-month-old rats used in the present study over the 14 days of the study. In a similar pattern, the plantaris wet weight of aged animals (33 months of age) was not different in animals killed at day 0 ($n$ = 4) from those killed after 14 days ($n$ = 4) of caged activity (−0.4% decrease).

Although we cannot rule out the possibility that a small reduction in the muscle mass of HS versus control animals was due to suppressed growth over 14 days, our data would suggest that this possibility is insufficient to explain our data. We make this conclusion because: (i) our pilot data show that the oldest animals do not grow significantly over 14 days (i.e., no muscle or body weight increases), and (ii) the increases in the muscle weight of the youngest animals in our pilot study were likely very modest and well below the 20% decrease in muscle mass due to HS in the young rats in the current study. Furthermore, our current data support the idea that muscle loss was due in part from increasing apoptotic signaling because there would be no reason to anticipate elevated apoptosis during a time of muscle growth. In fact, we have recently shown evidence that pro-apoptotic signaling decreases during periods of rapid muscle growth induced by overload (38,39). Thus, we interpret the data from our current study to indicate that HS induced "true" losses in muscle mass and not just a suppression of normal growth.

It was unexpected that the pro-apoptotic markers Apaf-1, AIF, and Id2 were greater in the aged plantaris muscle following HS even though the apoptotic index was not elevated. We favor the explanation that the increase in proapoptotic markers results in a cellular "environment" which is poised for apoptosis to occur, although this final step was not fully engaged during HS in aged plantaris muscles. One possible explanation for this discrepancy would be elevations in apoptotic inhibitor proteins, such as X-linked inhibitor of apoptosis protein (XIAP), which has been shown to increase to a greater extent in unloaded muscles of aged versus young adult birds, presumably as a means to offset apoptosis (38). An alternate explanation is that some of these pro-apoptotic markers may not always induce apoptosis just because they are present. For example, in addition to the subsequent cleavage and activation of pro-caspase-9 upon apoptosome formation with Apaf-1, caspase-9 can also be activated via an additional pathway independent of Apaf-1 in muscle cells (40,41). Furthermore, Apaf-1 is dispensable for apoptosis induced by cytotoxic drugs or overexpression of the transcription factor, E2F1, in primary myoblasts but not fibroblasts, whereas caspase-9 is required in both cell types (40). Finally, although cytoplasmic but not nuclear localization of Id2 is linked to apoptosis (42), Id2 also increases during periods of loading (39), and is associated with activation of satellite cells (43) to stimulate the anti-apoptotic event of muscle hypertrophy. Further work is needed to determine if unloading in aging muscles results in changes in the levels, compartmentalization, localization, or configuration of Id2 and/or other pro-apoptotic markers,

which may result in these markers having anti-apoptotic effects and offsetting the pro-apoptotic environment imposed by aging.

### Id2 and Apoptosis

Id2 is a negative regulator of basic helix–loop–helix proteins, including the myogenic regulatory factors MyoD and myogenin (32,33). The Id proteins bind to and sequester E-proteins, inhibiting myogenic regulatory factor binding and subsequent muscle-specific transcription. Data from our laboratory have led to the hypothesis of a dual role for Id2, based on the compartmentalization of Id2 within myocytes. In general, cytoplasmic Id2 appears to promote apoptotic processes and nuclear Id2 promotes proliferation and inhibits apoptosis through interactions with genes specific to these processes (32,42).

Our laboratory has previously demonstrated that increases in mRNA and protein levels of the Id proteins correlate with aging-associated muscle loss in the hind-limb muscles of aged rats (32,33). These findings have been extended in a model of unloading following stretch-overload-induced muscle hypertrophy (42). Cytoplasmic Id2 protein levels were higher in young unloaded patagialis (PAT) muscles compared to contralateral control muscles. Additionally, these increases in Id2 were positively correlated with other pro-apoptotic markers, such as Bax, AIF, p53, and the TUNEL index and negatively correlated with anti-apoptotic Bcl-2 (42). Thus, the subcellular partitioning of Id2 into the nucleus or the cytoplasm can lead to differential effects within skeletal muscle (42). Although these are correlational data and therefore do not show a cause-and-effect relationship between cytoplasmic Id2 and apoptosis, they do support previous data showing an association of Id2- and Bax-associated apoptosis (44). Indeed, the changes in Id2 mRNA observed in the current study were significantly correlated with changes in the pro-apoptotic markers Bax and caspase-9. These data add to the proposed ability of Id2 to promote apoptosis during aging and unloading, possibly through the caspase-dependent pathway.

### Summary

The results of the present study support the hypothesis that sarcopenia is associated with increases in markers supporting apoptosis and that nuclei of aged myocytes are susceptible to apoptosis. Additionally, we show that the fast plantaris muscles of aged rats responded differently to 2 weeks of HS when compared to young adult rats. Increases in Id2 mRNA were also noted in aged plantaris muscle following HS, supporting previous results (32,33), with positive correlations observed between Id2, Bax, and caspase-9. These results are consistent with the hypothesis that an increase in Id2 transcript levels, as observed with aging, may contribute to muscle mass losses in the aged plantaris muscle. In addition to these changes, an aging adaptation of skeletal muscle was identified in which anti-apoptotic Bcl-2 was up-regulated during unloading. These changes highlight the inherent differences between young and aged skeletal muscle and provide further evidence that apoptotic mechanisms are distinct with aging.

## Acknowledgments

The study was supported by the National Institutes of Health, National Institute on Aging grant R01AG021530.

Eva Engvall, PhD (La Jolla Cancer Research Foundation, La Jolla, CA) developed 2E8, and it was obtained from the Developmental Studies Hybridoma Bank developed under the auspices of the National Institute of Child Health and Human Development (NICHD) and maintained by the Department of Biological Sciences, The University of Iowa, Iowa City.

## References


1. Alway SE, Coggan AR, Sproul MS, Abduljalil AM, Robitaille PM. Muscle torque in young and older untrained and endurance-trained men. J Gerontol 1996;51A:B195–B201.
2. Daw CK, Starnes JW, White TP. Muscle atrophy and hypoplasia with aging: impact of training and food restriction. J Appl Physiol 1988;64:2428–2432. [PubMed: 3403425]
3. Degens H, Alway SE. Skeletal muscle function and hypertrophy are diminished at old age. Muscle Nerve 2003;27:339–347. [PubMed: 12635121]
4. Larsson L, Grimby G, Karlsson J. Muscle strength and speed of movement in relation to age and muscle morphology. J Appl Physiol 1979;46:451–456. [PubMed: 438011]
5. Wickham CC, Cooper C, Margetts BM, Barker DJ. Muscle strength, activity, housing, and the risk of falls in elderly people. Age Ageing 1989;18:47–51. [PubMed: 2565665]
6. Stump CS, Tipton CM, Henriksen EJ. Muscle adaptations to hindlimb suspension in mature and old Fischer 344 rats. J Appl Physiol 1997;82:1875–1881. [PubMed: 9173953]
7. Alley KA, Thompson LV. Influence of simulated bed rest and intermittent weight bearing on single skeletal muscle fiber function in aged rats. Arch Phys Med Rehabil 1997;78:19–25. [PubMed: 9014952]
8. Delp MD, Brown M, Laughlin MH, Hasser EM. Rat aortic vaso-reactivity is altered by old age and hindlimb unloading. J Appl Physiol 1995;78:2079–2086. [PubMed: 7665402]
9. Thompson LV, Brown M. Age-related changes in contractile properties of single skeletal fibers from aged soleus muscle. J Appl Physiol 1999;86:881–886. [PubMed: 10066700]
10. Chen KD, Alway SE. A physiological level of clenbuterol does not prevent atrophy or loss of force in skeletal muscle of old rats. J Appl Physiol 2000;89:606–612. [PubMed: 10926644]
11. Allen DL, Linderman JK, Roy RR, et al. Apoptosis: a mechanism contributing to remodeling of skeletal muscle in response to hindlimb unweighting. Am J Physiol 1997;273:C579–C587. [PubMed: 9277355]
12. Alway SE, Lowe DA, Chen KD. The effects of age and hindlimb suspension on the levels of expression of the myogenic regulatory factors MyoD and myogenin in rat fast and slow skeletal muscles. Exp Physiol 2001;86:509–517. [PubMed: 11445830]
13. Chen KD, Alway SE. Clenbuterol reduces soleus muscle fatigue during disuse in aged rats. Muscle Nerve 2001;24:211–222. [PubMed: 11180204]
14. Thompson LV, Johnson SA, Shoeman JA. Single soleus muscle fiber function after hindlimb unweighting in adult and aged rats. J Appl Physiol 1998;84:1937–1942. [PubMed: 9609787]
15. Thomason DB, Booth FW. Atrophy of the soleus muscle by hindlimb suspension. J Appl Physiol 1990;68:1–12. [PubMed: 2179205]
16. Fitts RH, Metzger JM, Riley DA, Unsworth BR. Models of disuse: a comparison of hindlimb suspension and immobilization. J Appl Physiol 1986;60:1946–1953. [PubMed: 3722061]
17. Morey-Holton ER, Globus RK. Hindlimb unloading rodent model: technical aspects. J Appl Physiol 2001;92:1367–1377. [PubMed: 11895999]
18. Price SR, Mitch WE. Mechanisms stimulating protein degradation to cause muscle atrophy. Curr Opin Clin Nutr Metab Care 1998;1:79–83. [PubMed: 10565334]
19. Zarzhevsky N, Menashe O, Carmeli E, Stein H, Reznick AZ. Capacity for recovery and possible mechanisms in immobilization atrophy of young and old animals. Ann N Y Acad Sci 2001;928:212–225. [PubMed: 11795512]
20. McDonald KS, Blaser CA, Fitts RH. Force-velocity and power characteristics of rat soleus muscle fibers after hindlimb suspension. J Appl Physiol 1994;77:1609–1616. [PubMed: 7836176]
21. Allen DL, Roy RR, Edgerton VR. Myonuclear domains in muscle adaptation and disease. Muscle Nerve 1999;22:1350–1360. [PubMed: 10487900]
22. Hikida RS, Van Nostran S, Murray JD, Staron RS, Gordon SE, Kraemer WJ. Myonuclear loss in atrophied soleus muscle fibers. Anat Rec 1997;247:350–354. [PubMed: 9066912]
23. Fauteck SP, Kandarian SC. Sensitive detection of myosin heavy chain composition in skeletal muscle under different loading conditions. Am J Physiol 1995;268:C419–C424. [PubMed: 7864081]

24. Leeuwenburgh C, Gurley CM, Strotman BA, Dupont-Versteegden EE. Age-related differences in apoptosis with disuse atrophy in soleus muscle. Am J Physiol 2005;288:R1288–R1296.
25. Siu PM, Pistilli EE, Alway SE. Apoptotic responses to hindlimb suspension in gastrocnemius muscles from young and aged rats. Am J Physiol 2005;289:R1015–R1026.
26. Ohira Y, Yoshinaga T, Nomura T, et al. Gravitational unloading effects on muscle fiber size, phenotype, and myonuclear number. Adv Space Res 2002;30:777–781. [PubMed: 12530363]
27. Adams V, Gielen S, Hambrecht R, Schuler G. Apoptosis in skeletal muscle. Front Biosci 2001;6:1–11.
28. Li P, Nijhawan D, Budihardjo L, et al. Cytochrome c and dATP-dependent formation of Apaf-1/caspase-9 complex initiates an apoptotic protease cascade. Cell 1997;91:479–489. [PubMed: 9390557]
29. Zou H, Li Y, Liu X, Wang X. An Apaf-1-cytochrome c multimeric complex is a functional apoptosome that activates pro-caspase-9. J Biol Chem 1999;274:11549–11556. [PubMed: 10206961]
30. Daugas E, Nochy D, Ravagnan L, et al. Apoptosis-inducing factor (AIF): a ubiquitous mitochondrial oxidoreductase involved in apoptosis. FEBS Lett 2000;476:118–123. [PubMed: 10913597]
31. Susin SA, Zamzami N, Castedo M, et al. Bcl-2 inhibits the mitochondrial release of an apoptogenic protease. J Exp Med 1996;184:1331–1341. [PubMed: 8879205]
32. Alway SE, Degens H, Krishnamurthy G, Smith CA. Potential role for Id myogenic repressors in apoptosis and attenuation of hypertrophy in muscles of aged rats. Am J Physiol 2002;283:C66–C76.
33. Alway SE, Degens H, Lowe DA, Krishnamurthy G. Increased myogenic repressor Id mRNA and protein levels in hindlimb muscles of aged rats. Am J Physiol 2002;282:R411–R422.
34. Dirks A, Leeuwenburgh C. Apoptosis in skeletal muscle with aging. Am J Physiol 2002;282:R519–R527.
35. Pollack M, Phaneuf S, Dirks A, Leeuwenburgh C. The role of apoptosis in the normal aging brain, skeletal muscle, and heart. Ann N Y Acad Sci 2002;959:93–107. [PubMed: 11976189]
36. Rothermel B, Vega RB, Yang J, Wu H, Bassel-Duby R, Williams RS. A protein encoded within the Down syndrome critical region is enriched in striated muscles and inhibits calcineurin signaling. J Biol Chem 2000;24:8719–8725. [PubMed: 10722714]
37. Siu PM, Pistilli EE, Butler DC, Alway SE. Aging influences cellular and molecular response of apoptosis to skeletal muscle unloading. Am J Physiol 2005;288:C338–C349.
38. Siu PM, Pistilli EE, Ryan MJ, Alway SE. Aging sustains the hypertrophy-associated elevation of apoptotic suppressor X-linked inhibitor of apoptosis protein (XIAP) in skeletal muscle during unloading. J Gerontol Biol Sci Med Sci 2005;60A:976–983.
39. Siu PM, Alway SE. Subcellular responses of p53 and Id2 in fast and slow skeletal muscle in response to stretch-induced overload. J Appl Physiol 2005;99:1897–1904. [PubMed: 16002773]
40. Ho AT, Li QH, Hakem R, Mak TW, Zacksenhaus E. Coupling of caspase-9 to Apaf-1 in response to loss of pRb or cytotoxic drugs is cell-type-specific. EMBO J 2004;23:460–472. [PubMed: 14713951]
41. Ho AT, Zacksenhaus E. Splitting the apoptosome. Cell Cycle 2004;3:446–448. [PubMed: 15020840]
42. Siu PM, Alway SE. Id2 and p53 participate in apoptosis during unloading-induced muscle atrophy. Am J Physiol 2005;288:C1058–C1073.
43. Alway SE, Martyn JK, Ouyang J, Chaudhrai A, Murlasits ZS. Id2 expression during apoptosis and satellite cell activation in unloaded and loaded quail skeletal muscles. Am J Physiol 2003;284:R540–R549.
44. Florio M, Hernandez MC, Yang H, Shu HK, Cleveland JL, Israel MA. Id2 promotes apoptosis by a novel mechanism independent of dimerization to basic helix-loop-helix factors. Mol Cell Biol 1998;18:5435–5444. [PubMed: 9710627]

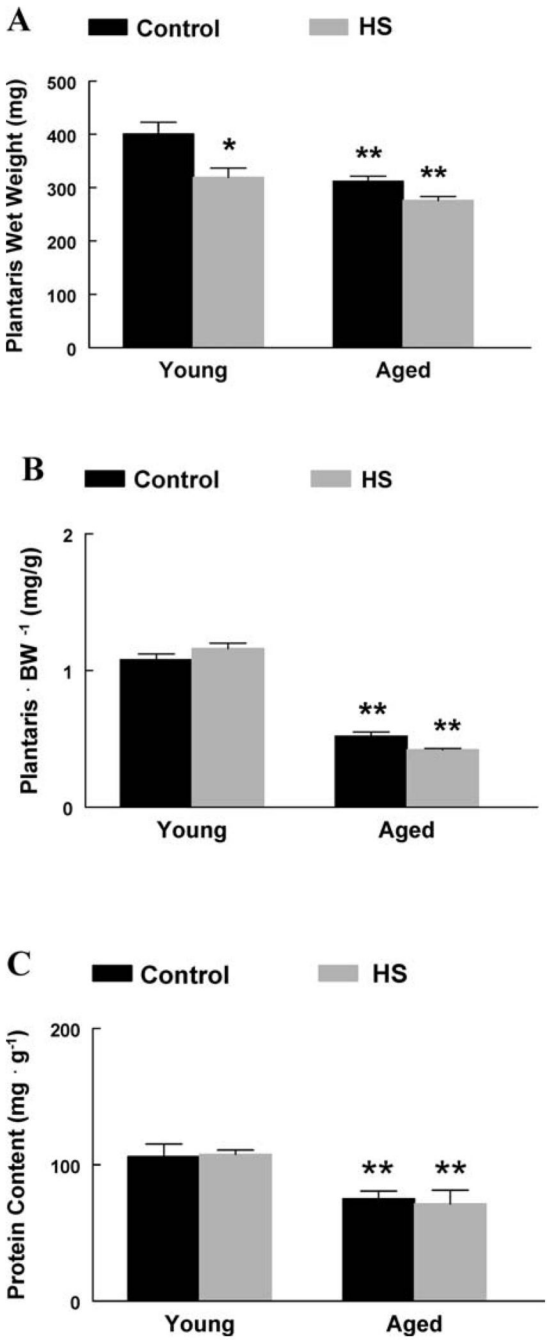


**Figure 1.**

**A**, Absolute plantaris muscle wet weight. Plantaris muscles from young and aged animals expressed as milligrams of tissue. *Significant effect of hind-limb suspension (HS; $p < .05$). **Significant effect of aging ( $p < .05$). Data are presented as means ± standard error (*SE*). **B**, Normalized plantaris muscle weight (mg · g $^{-1}$). Plantaris muscles from young and aged animals were normalized to the animal body weight in grams. **Significant effect of aging ( $p < .05$). Data are presented as means ± *SE*. **C**, Plantaris muscle protein content (mg · g $^{-1}$). Plantaris protein content was determined in young and aged plantaris muscles following HS. **Significant effect of aging ( $p < .05$). Data are presented as means ± *SE*.

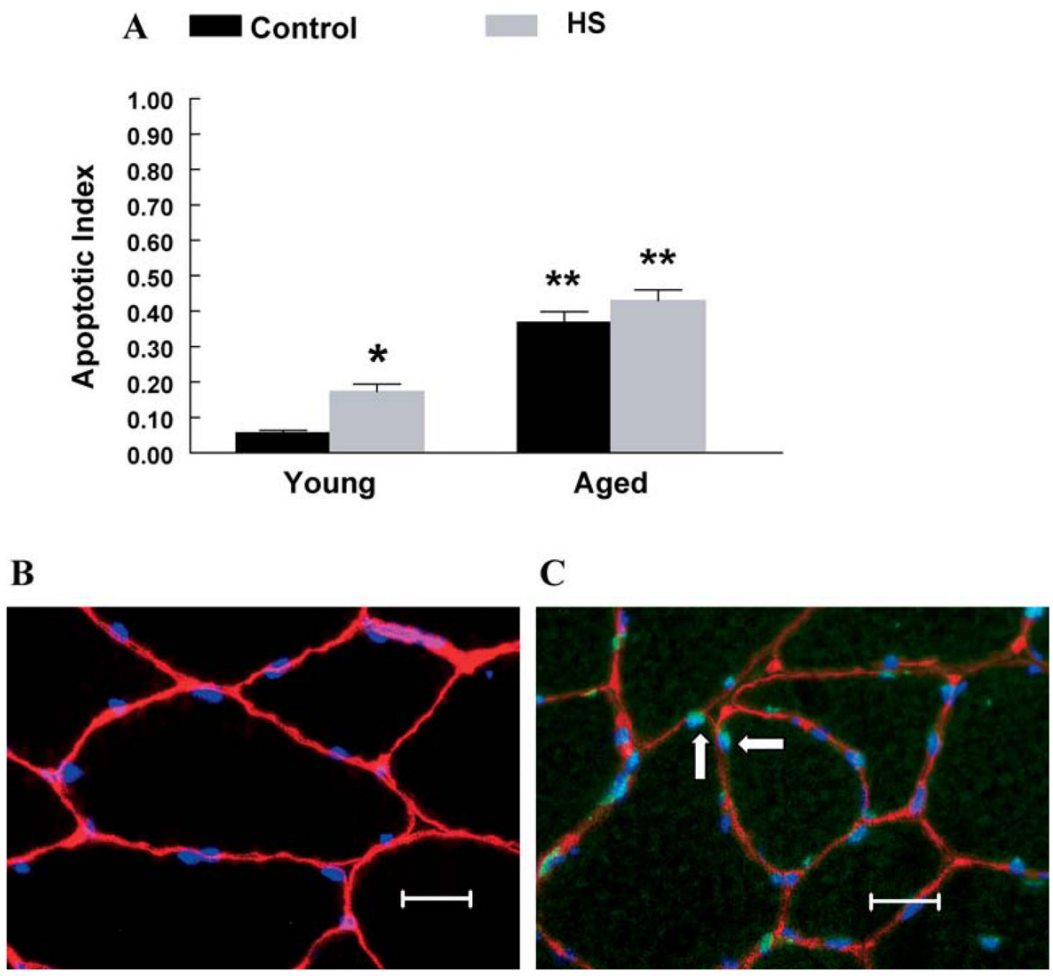


**Figure 2.**

**A**, Apoptotic index (optical density [OD] 405 · mg protein$^{-1}$). The extent of DNA fragmentation was assayed using a cell death enzyme-linked immunosorbent assay (ELISA) kit. *Significant effect of hind-limb suspension (HS; $p < .05$). **Significant effect of aging ( $p < .05$). Data are presented as means ± standard error (*SE*). **B**, Fluorescent terminal deoxynucleotidyl transferase biotin-dUTP nick end labeling (TUNEL) stain in young control muscle. TUNEL staining was used to determine the extent of nuclear apoptosis in gastrocnemius muscles from young animals. Muscle fiber borders were visualized using a rat laminin antibody, and nonapoptotic nuclei were visualized using 4′,6-diamidino-2-phenylindole (DAPI). The image was obtained at an objective magnification of 40×. Bar, 10 μm. **C**, Fluorescent TUNEL stain in aged control muscle. TUNEL staining was used to determine the extent of nuclear apoptosis in gastrocnemius muscles from old animals. Muscle fiber borders were visualized using a rat laminin antibody. All nuclei were stained with DAPI. Arrows highlight TUNEL-positive nuclei. Nonapoptotic nuclei were TUNEL negative. The image was obtained at an objective magnification of 40×. Bar, 10 μm.

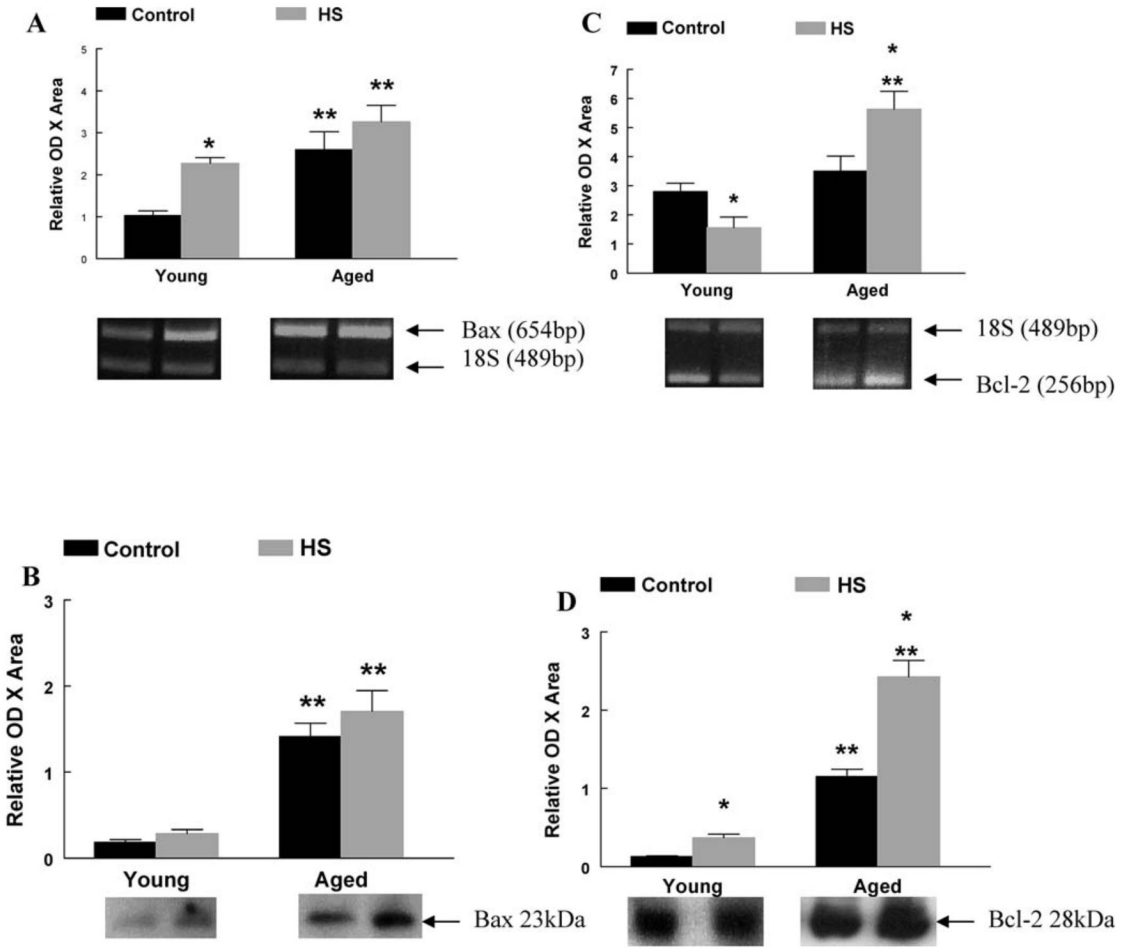


**Figure 3.**

**A**, Bax messenger RNA (mRNA). The mRNA content for pro-apoptotic Bax was determined by reverse transcription–polymerase chain reaction (RT–PCR), with PCR products normalized to the 18S gene. Representative agarose gel images following electrophoresis are displayed for each group. *Significant effect of hind-limb suspension (HS; $p < .05$). **Significant effect of aging ( $p < .05$). Data are presented as means ± standard error (*SE*). **B**, Bax protein content. The protein content of pro-apoptotic Bax was determined by western immunoblot. Representative blots following antibody incubation are displayed. **Significant effect of aging ( $p < .05$). Data are presented as means ± *SE*. **C**, Bcl-2 mRNA. The mRNA content for anti-apoptotic Bcl-2 was determined by RT–PCR, with PCR products normalized to the 18S gene. Representative agarose gel images following electrophoresis are displayed for each group. *Significant effect of HS ( $p < .05$). **Significant effect of aging ( $p < .05$). Data are presented as means ± *SE*. **D**, Bcl-2 protein content. The protein content of anti-apoptotic Bcl-2 was determined by western immunoblot. Representative blots following antibody incubation are displayed. *Significant effect of HS ( $p < .05$). **Significant effect of aging ( $p < .05$). Data are presented as means ± SE.

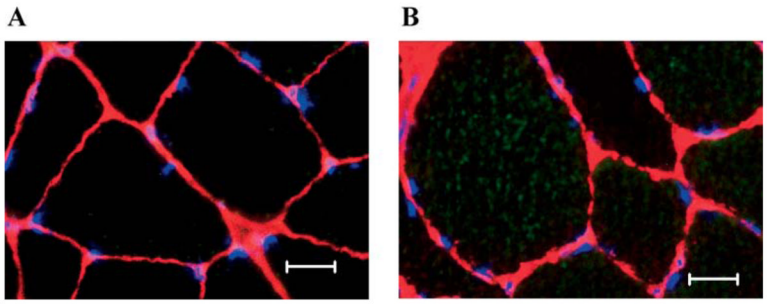


**Figure 4.**

**A**, Fluorescent image of Bax protein in young control muscle. The extent of cytoplasmic Bax protein was determined using fluorescence microscopy. A faint Bax stain was visualized in gastrocnemius muscles from young animals. Muscle fiber borders were visualized using a rat laminin antibody, and nonapoptotic nuclei were visualized using 4′,6-diamidino-2-phenylindole (DAPI). The image was obtained at an objective magnification of 40×. Bar, 10 μm. **B**, Fluorescent image of Bax protein in aged control muscle. The extent of cytoplasmic Bax protein was determined using fluorescence microscopy. Bax protein was visualized throughout the cytoplasm of aged muscle fibers. Muscle fiber borders were visualized using a rat laminin antibody, and nonapoptotic nuclei were visualized using DAPI. The image was obtained at an objective magnification of 40×. Bar, 10 μm.

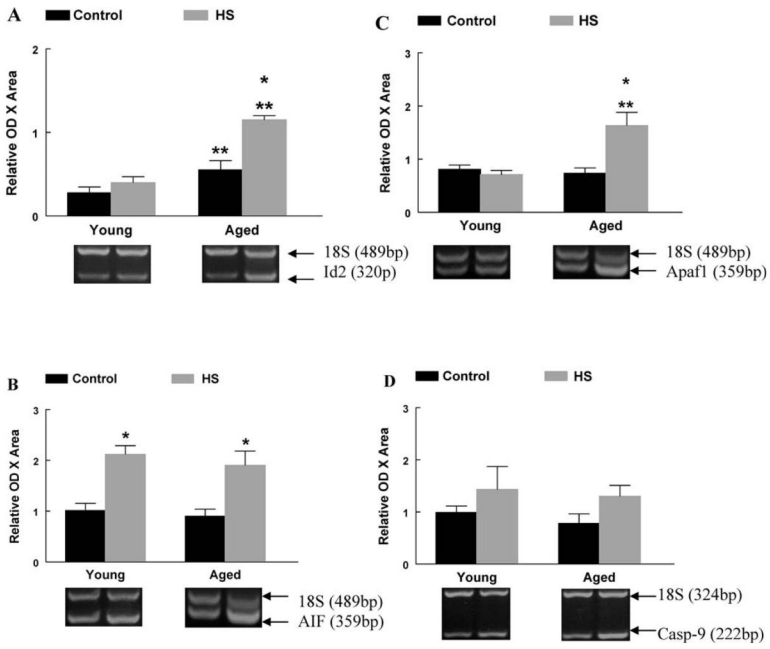


**Figure 5.**

**A**, Inhibitor of differentiation protein-2 (Id2) messenger RNA (mRNA). The mRNA content for Id2 was determined by reverse transcription–polymerase chain reaction (RT–PCR), with PCR products normalized to the 18S gene. Representative agarose gel images following electrophoresis are displayed for each group. *Significant effect of hind-limb suspension (HS; $p < .05$). **Significant effect of aging ( $p < .05$). Data are presented as means ± standard error (*SE*). **B**, Apoptosis-inducing factor (AIF) mRNA. The mRNA content for AIF was determined by RT–PCR, with PCR products normalized to the 18S gene. Representative agarose gel images following electrophoresis are displayed for each group. **Significant effect of aging ( $p < .05$). Data are presented as means ± *SE*. **C**, Apaf-1 mRNA. The mRNA content for Apaf-1 was determined by RT–PCR, with PCR products normalized to the 18S gene. Representative agarose gel images following electrophoresis are displayed for each group. *Significant effect of HS ( $p < .05$). **Significant effect of aging ( $p < .05$). Data are presented as means ± *SE*. **D**, Caspase-9 mRNA. The mRNA content for caspase-9 was determined by RT–PCR, with PCR products normalized to the 18S gene. Representative agarose gel images following electrophoresis are displayed for each group. Data are presented as means ± *SE*.

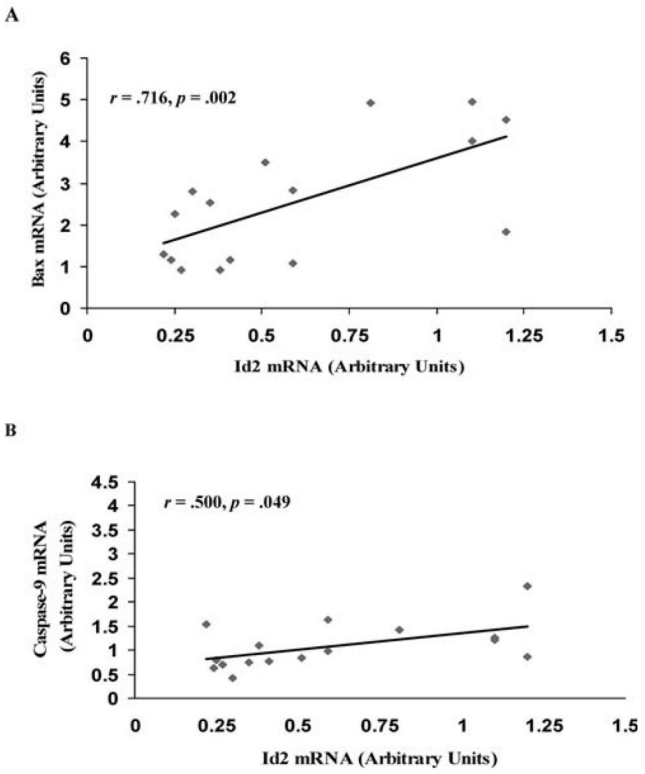


**Figure 6.**

**A**, Correlational analysis of Bax and inhibitor of differentiation protein-2 (Id2) messenger RNA (mRNA). The relationship between the changes in Bax mRNA and Id2 mRNA were determined by calculating the Pearson correlation coefficient. **B**, Correlational analysis of caspase-9 and Id2 mRNA. The relationship between the changes in caspase-9 mRNA and Id2 mRNA were determined by calculating the Pearson correlation coefficient.

**Table 1**

Primers Used for Polymerase Chain Reaction (PCR) Amplifications of Complementary DNA

| Product | Accession No. | Sequence | Position | $T_A$ °C | PCR Length (bp) | Restriction Enzyme | Restriction Products (bp) |
|---|---|---|---|---|---|---|---|
| Id2 | NM_013060 | F: 5′-GAATTCTCAGCATGAAAGCTTTCAGCC-3′<br>R: 5′-CTCGAGATTCAGCCACAGAGCGCT-3′ | 365–385<br>664–684 | 52.7 | 320 | *Alu*I | 262, 68 |
| Apaf-1 | AF218388 | F: 5′-CGGCCCTGCGCATCTGATTCAT-3′<br>R: 5′-GGGCGAACGACTAAGCGGGACAG-3′ | 1623–1644<br>1888–1910 | 57.8 | 288 | *Alu*I | 193, 95 |
| AIF | AF375656 | F: 5′-CCGGCTTCCAGGCAACTTGTTCC-3′<br>R: 5′-CCCGGATGGATCTAGCTGCTGCA-3′ | 93–115<br>429–451 | 58.1 | 359 | *Kpn*I | 290, 69 |
| Caspase 9 | NM_031632 | F: 5′-GGCCGGTGGACATTGGTTCTGG-3′<br>R: 5′-CCATGAAGCGCAGCCAGCAGAA-3′ | 543–564<br>743–764 | 60.1 | 222 | *Bam*HI | 130, 92 |
| Bax | AF235993 | F: 5′-GCACCCCTTTCCTCCTCTCTCCACCAG-3′<br>R: 5′-TGCCTTTCCCCGTTCCCCATTCATC-3′ | 462–488<br>1091–1115 | 55 | 654 | *Bam*HI<br>*Bst*XI | 445, 209<br>521, 133 |
| Bcl-2 | U34964 | F: 5′-CGGGCTGGGGATGACTTCTCTC-3′<br>R: 5′-GCCGGTTCAGGTACTCAGTCAT-3′ | 286–307<br>520–541 | 59.1 | 256 | *Alu*I | 196, 60 |

*Note*: $T_A$ = annealing temperature; Id2 = inhibitor of differentiation protein 2; Apaf-1 = apoptotic protease activating factor 1; AIF = apoptosis-inducing factor; F = forward; R = reverse.